Restructuring of *hex*-Pt(100) under CO gas environments: formation of 2-D nanoclusters

Feng Tao, Sefa Dag, Lin-Wang Wang, Zhi Liu, Derek Butcher, Miquel Salmeron, Gabor A. Somorjai**

Department of Chemistry. University of California, Berkeley
Materials Sciences Divisions, Lawrence Berkeley National Laboratory, Berkeley, CA 94720
Advanced Light Sources, Lawrence Berkeley National Lab, Berkeley, CA 94720
Computational Research Division, Lawrence Berkeley National Laboratory, Berkeley, California 94720

Abstract

The atomic-scale restructuring of *hex*-Pt(100) induced by carbon monoxide with a wide pressure range was studied with a newly designed chamber-in-chamber high-pressure STM and theoretical calculations. Both experimental and DFT calculation results show that CO molecules are bound to Pt nanoclusters through a tilted on-top configuration with a separation of ~3.7-4.1 Å. The phenomenon of restructuring of metal catalyst surfaces induced by adsorption, and in particular the formation of small metallic clusters suggests the importance of studying structures of catalyst surfaces under high pressure conditions for understanding catalytic mechanisms.

*Corresponding authors: email: Somorjai@berkeley.edu, MBSalmeron@lbl.gov

The ability of surfaces to restructure under the influence of adsorbates, plays a crucial role in heterogeneous catalysis because catalytic activity and selectivity depend strongly on the arrangement of metal atoms that form active sites [1]. Catalytic reactions take place in the presence of reactant gases at pressures ranging from mTorr to atmospheres and under these conditions dense layers of adsorbed molecules form with structures determined both by thermodynamics and kinetics. The pressure-dependent entropy, kT·*log*P, significantly contributes to the Gibbs free energy of the system and may result in a surface structure different from that at low pressure[2, 3]. Particularly important are reconstructions that might generate structures unstable under vacuum or under low pressure conditions. For these reasons, studies using techniques that can operate under relevant gas pressures are highly desirable. Scanning tunneling microscopy (STM) can provide atomic resolution images of surfaces over a wide pressure range of reactants. A new high-pressure STM operating inside a small volume reaction cell was built in our laboratory and used in the present study.[4]

The Pt(100) surface is interesting because its stable structure consists of a *quasi*-hexagonal overlayer, or *hex*-Pt(100), on top of the square symmetry (100) lattice[5]. Similar reconstructions have been observed on the (100) surfaces of other 5d transition metals such as Au and Ir under high vacuum[6]. Figures 1a and 1b show schematically the structure of the *hex*-Pt(100) surface. Six rows of atoms in the top layer span the width of five rows of atoms of the underlying (1×1) plane along the [011] direction. This structure contains ~20% more Pt atoms than the bulk terminated (1×1) layer[5, 6]. Interestingly, the hexagonal reconstruction is not observed on the 4d metals including Rh, Pd, and Ag. The criterion for this reconstruction has been explained as the result of the balance between electronic and elastic surface-substrate mismatch energies [7]. The electronic part originates from the depletion of *d*-electrons in the surface atoms resulting in a reduced anti-bonding contribution at the surface. Only the three late 5d metals have enough electronic energy gain to counter balance the elastic resistance of the substrate to lattice mismatch and thus reconstruct[7].

Several studies have shown that chemisorbed gases, including CO [8-15], NO [16], O_2 [17, 18], and C_2H_4 [19] can lift the reconstruction so that the top Pt atoms form again a square bulk-like structure under the chemisorbed species[8, 13-15]. Most of these studies were performed using low energy electron diffraction (LEED) under high vacuum conditions.

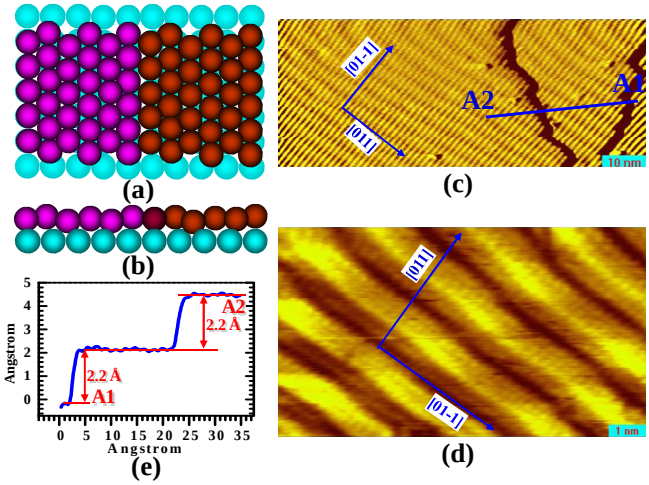

Figure 1. (a) and (b) Schematic diagram of the *quasi*-hexagonal layer on the Pt(100) surface. The diagrams (a) and (b) show top and side views, respectively. The Pt atoms of the unreconstructed (1×1) bulk plane are represented by light balls. (c) STM image showing parallel bands along [011] direction spaced by 5 Pt atoms distances. (d) High resolution image of the *hex*-Pt(100) surface. (e) Line-profile along A1-A2 in (c).

LEED provides crystallographic information of the ordered part of the surface when the domain dimensions are larger than the coherence length of the electron beam. Very small domains, like the islands produced by restructuring the Pt(100) object of this study, would give rise to broadened diffraction spots that make crystallographic analysis of their structure difficult. In addition, in most cases the surfaces were examined in ultrahigh vacuum after pumping away the CO gas phase, which results in desorption of some of the adsorbed CO molecules. STM however does not suffer from the limitations of diffraction, and can be used to study the surface structure of *hex*-Pt(100) in the presence of the CO gas at pressures ranging from 10^{-9} to several Torr at room temperature.

A clean *hex*-Pt(100) surface was prepared by cycles of sputtering at 700 eV Ar^+, annealing to ~950 K in 2×10^{-7} Torr O_2, and annealing in UHV at ~1100 K. A final annealing in UHV was carried out at ~1130 K followed by slow cooling to room temperature. Surface cleanliness was checked with Auger Electron Spectroscopy and STM. The new STM instrument used in this study is enclosed in a reactor

cell with a volume of ~19 cm^3 and offers the capability of working from UHV to ten bars as well as providing in-situ heating of the sample[4].

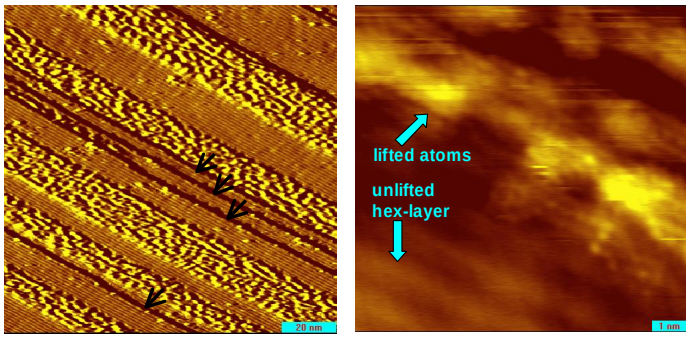

Figure 2. (a) Large-scale image of Pt(100) in an environment of 5×10^{-9} Torr CO. Step edges are marked with arrows. The surface reconstruction is only partially lifted, giving rise to clusters of Pt atoms aligned along the [01-1] direction. (b) High resolution image showing areas of lifted and unlifted atoms in the same terrace.

Figure 2 shows an STM image obtained in CO at pressures between 10^{-9} and 10^{-8} Torr. At these pressures the surface is only partially reconstructed with the lifted atoms forming clusters along the [110] direction in the same terrace.

Figure 3 is a large-scale STM image of Pt(100) in an environment of ~10^{-5} Torr of CO, showing numerous islands of 0.5 to 3.5 nm in size and ~0.23 nm high. The entire surface is now restructured and no stripes characteristic of the 5 × n (n=20 or 14) unit-cell of *hex*-Pt(100) are visible. The islands are formed by the Pt atoms segregated from the top layer after restructuring induced by chemisorbed CO.

More information was obtained from analysis of high-resolution images acquired under CO pressures ranging from 10^{-6} to several Torr, as in the example of Figure 4a. Each island consists of an approximately square arrangement of maxima along both the [01-1] and [011] directions with a corrugation of ~ 0.1 nm. The area occupied by the islands is ~45% of the total area, much larger than the 20% expected from the density of the hexagonal reconstructed surface layer. Equally surprising is the large distance between the maxima, between 0.37 and 0.40 nm, which is 1.34 to 1.44 times the 0.28 nm distance between neighboring Pt atoms in the bulk. By counting maxima in these images we obtain a number density of ~23%, close to the number expected from the extra density of atoms in the *hex*-

overlayer. Thus, it is the large distance between maxima that explains how 20% excess of Pt atoms can form islands covering 45% of the total area.

The nearly square arrangement of Pt atoms in the islands is different from the c(2×2) structure observed by LEED after exposing the Pt(100) to CO [9, 10, 13-15]. The structure revealed by LEED refers to the large coherent domains between the small islands. STM on the other hand sees only the top of the islands which, because of their small size contribute mostly to the background in the diffraction pattern. Unfortunately the finite radius of the tip apex and the noise level (a few tens of pm) prevented obtaining high resolution images of the areas between the islands.

The large separation (0.37-0.40 nm) between maxima in the islands may be explained by the steric hindrance from repulsion between CO molecules that prevents them from getting closer than roughly their van der Waals diameter. Two models can be proposed to accommodate the repulsion. In one model CO-Pt atom moieties are separated by the CO diameter, with the Pt atoms out of registry with the substrate. A second model calls for the formation of very small islands, with the Pt atoms on lattice sites. The island size must be limited to roughly 3 atoms so that the CO molecules can fan out, those at the edges tilting farther away from the center. There is an energy penalty due to loss of coordination of the Pt atoms with the substrate in the first model, while the molecular compression and tilting increases the energy in the second model.

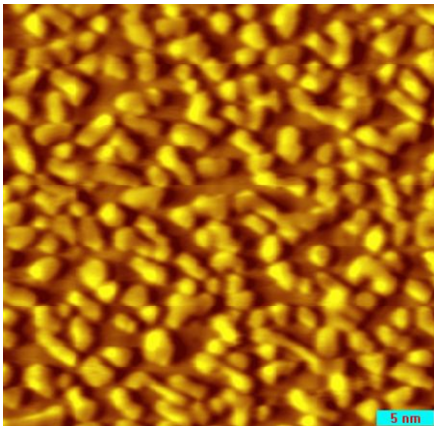

Figure 3. 38×36 nm STM image of the Pt(100) surface after restructuring induced by adsorbed CO in equilibrium with the gas at 10^{-5} Torr. Numerous islands are formed by Pt atoms expelled from the hexagonal structure. The islands cover ~45% area of the surface.

To gain a deeper understanding of the cluster stability we performed density functional theory (DFT) calculations using a Pt(100) slab with a Pt cluster on top. The calculations were performed in the generalized gradient approximation PW91 functional[20], within a plane-wave pseudo-potential scheme using the Vienna ab-initio Simulation Package[21]. We used Projector Augmented Wave pseudopotentials[22] and an energy cutoff at 400 eV for plane wave expansion. Uniform grids of k-points were obtained using the Monkhorst-Pack scheme [23] of 2×4×1 k-point meshes for the slab calculation.

The initial geometry of the cluster was an array of 3×6 atoms spaced by 0.37 nm on top of a 4×8 (1×1) substrate, as shown in Figure 5a. In our calculations we used a slab consisting of six layers of Pt atoms and a top Pt layer (dark and light blue circles in Figure 5). The first 5 layers of the slab are fixed with the DFT calculated bulk constant, while the 6th layer together with the additional top Pt layer are allowed to relax. After relaxation however, the Pt atoms in the cluster migrated to 4-fold lattice sites of the bulk termination. In addition, the cluster split into two 3×3 clusters separated by two Pt lattice distances and with the CO molecules tilted away from each other at the edges (Figure 5b). The stabilization energy gained from this rearrangement is 3.2 eV per Pt-CO pair, which lends strong support to the second model. The resulting spacing of the O end of the CO molecules varies from 0.37 to 0.41 nm. Within the Tersoff-Hamman approximation, which models the STM contrast, the calculated corrugation profile for an electron density of 1×10^{-3} nm^{-3} at the Fermi level in the optimized 3×3 cluster is 0.11 nm over CO, and 0.01 nm over bare Pt in the 1×1 structure, (Figure 5c), in good agreement with the experimental measurements. Due to the molecular tilt, adjacent clusters separated by 2 Pt-Pt distances appear in the STM images as a contiguous cluster.

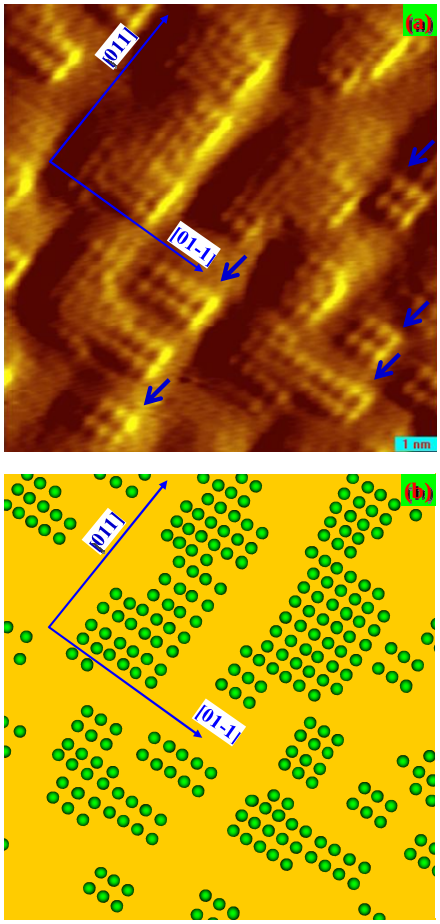

Figure 4. (a) Atomically resolved image (10 × 10 nm) of the islands formed in 10^{-6} Torr CO. (b) Schematic representation of the image, each dot corresponding to a maximum in the top image.

The interesting conclusion from these results is that the strong binding energy of CO to the Pt atoms together with the repulsion between the molecules drives a restructuring of the metal substrate, breaking islands into smaller entities that maximize bonding of more CO molecules.

Previous STM studies have shown that CO molecules on Pt(111) form a Moiré overlayer with a pressure-dependent coverage of 0.5-0.65 in the pressure range of 10^{-6} – 760 Torr [24, 25]. In this overlayer the molecules do not occupy high-symmetry sites but form an incommensurate hexagonal arrangement with variable adsorption sites. On the small islands formed after reconstruction of the compact *hex*-Pt(100) layer, the overlayer is not incommensurate but the molecules adopt a tilted on-top binding dictated by their repulsion.

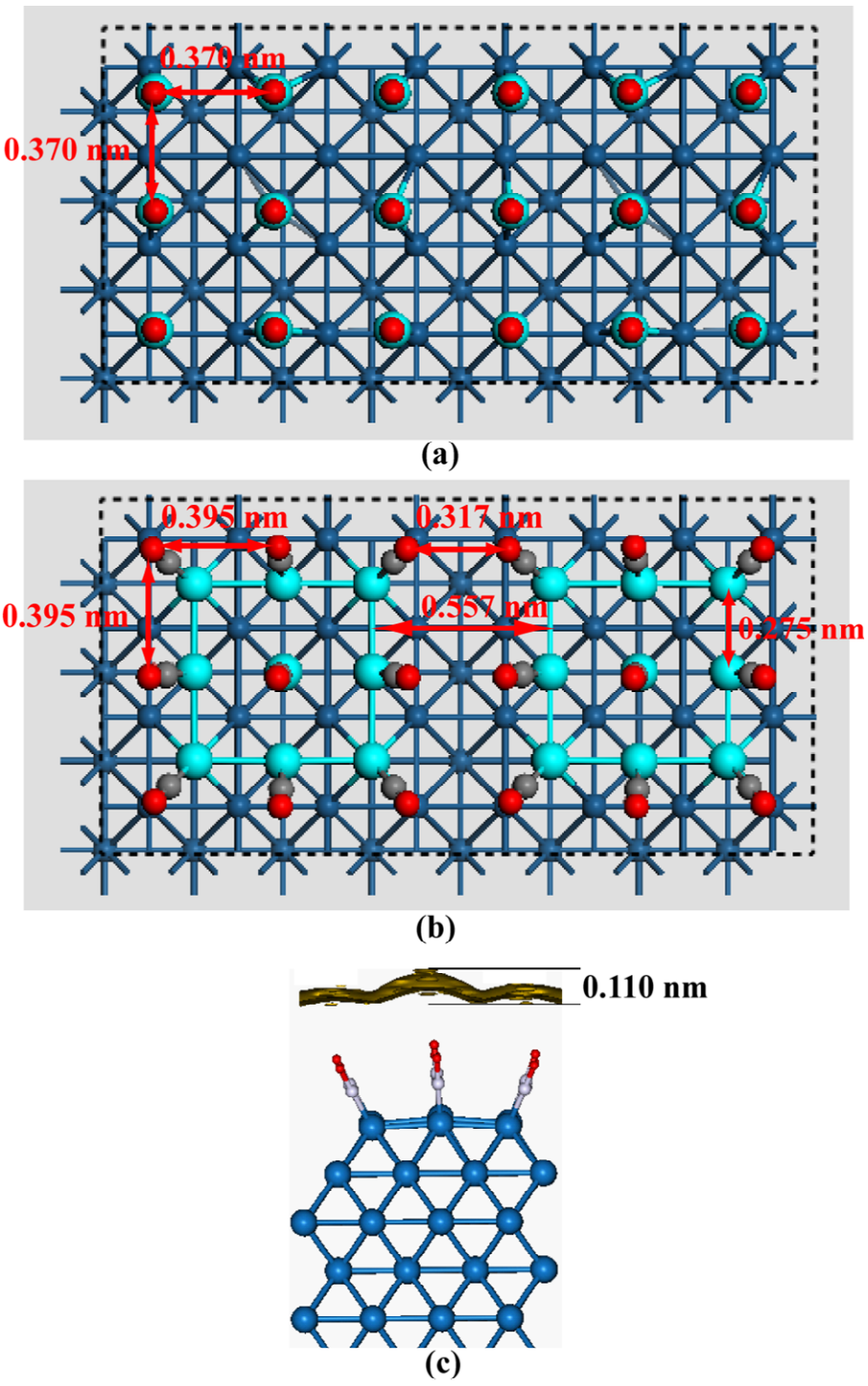

Figure 5. (a) Starting geometry of CO and Pt atoms forming a (6 × 3) cell before relaxation. The Pt atoms and CO molecules are separated by 0.37 nm as the maxima in the STM images. (b) After relaxation to minimize energy in the DFT calculation two (3 × 3) clusters are formed. The average Pt-Pt distance in the new clusters is 0.275 nm, as in the bulk, while the average O-O distance from the CO molecules is 0.37-0.41 nm, which matches the experimental findings. The distance between the nearest oxygen atoms of the two (3 × 3) clusters is 0.32 nm. This relaxed geometry is the stable one. (c) Calculated corrugation of the electron density profile at the Fermi level of the optimized 3×3 cluster. In (a) and (b), the dark blue circles represent platinum atoms in the slab layers, whereas the light blue circles represent Pt atoms at the surface. The red and gray circles represent oxygen and carbon atoms respectively.

In summary, we have studied the atomic scale restructuring of the *hex*-Pt(100) surface induced by CO in a wide pressure range of gas environments. Both experimental and theoretical results show that the CO molecules are bound to small Pt nanoclusters in a tilted on-top configuration. The phenomenon of restructuring of metal catalyst surfaces induced by adsorption, and in particular the formation of small metallic clusters opens a new avenue for understanding catalytic activity under high pressures, a concept that only structural studies in the presence of gases can reveal.

Acknowledgements

This work was supported by the director of the Office of Science, Office of Basic Energy Sciences, Materials Sciences and Engineering; and Chemical Sciences, by the Office of Advanced Scientific Computing Research; Geosciences, and by the Biosciences Division of the U.S. Department of Energy under contract DE-AC02-05CH11231. The computation of this work used the resource of the National Energy Research Scientific Computing Center (NERSC)

References

1. Somorjai, G. A., *Introduction to Surface Chemistry and Catalysis*. Wiley VCH: 1999; p 442.
2. Salmeron, M.; Schlogl, R. *Surface Science Reports* **2008,** 63, (4), 169-199.
3. Over, H.; Muhler, M. *Progress in Surface Science* **2003,** 72, (1-4), 3-17.
4. Tao, F.; Tang, D.; Salmeron, M.; Somorjai, G. A. *Reivew of Scientific Instruments* **2008,** 79, 084101.
5. Hagstrom, S.; Lyon, H. B.; Somorjai, G. A. *Physical Review Letters* **1965,** 15, (11), 491-&.
6. Vanhove, M. A.; Koestner, R. J.; Stair, P. C.; Biberian, J. P.; Kesmodel, L. L.; Bartos, I.; Somorjai, G. A. *Surface Science* **1981,** 103, (1), 189-217.
7. Fiorentini, V.; Methfessel, M.; Scheffler, M. *Physical Review Letters* **1993,** 71, (7), 1051-1054.
8. Ritter, E.; Behm, R. J.; Potschke, G.; Wintterlin, J. *Surface Science* **1987,** 181, (1-2), 403-411.
9. Behm, R. J.; Thiel, P. A.; Norton, P. R.; Ertl, G. *Journal of Chemical Physics* **1983,** 78, (12), 7437-7447.
10. Thiel, P. A.; Behm, R. J.; Norton, P. R.; Ertl, G. *Journal of Chemical Physics* **1983,** 78, (12), 7448-7458.
11. Chang, C. S.; Su, W. B.; Tsong, T. T. *Surface Science* **1995,** 330, (3), L686-L690.
12. Borg, A.; Hilmen, A. M.; Bergene, E. *Surface Science* **1994,** 306, (1-2), 10-20.
13. Norton, P. R.; Davies, J. A.; Creber, D. K.; Sitter, C. W.; Jackman, T. E. *Surface Science* **1981,** 108, (2), 205-224.

14. Davies, J. A.; Norton, P. R. *Nuclear Instruments & Methods* **1980,** 168, (1-3), 611-615.
15. Helms, C. R.; Bonzel, H. P.; Kelemen, S. *Journal of Chemical Physics* **1976,** 65, (5), 1773-1782.
16. Mase, K.; Murata, Y. *Surface Science* **1992,** 277, (1-2), 97-108.
17. Griffiths, K.; Jackman, T. E.; Davies, J. A.; Norton, P. R. *Surface Science* **1984,** 138, (1), 113-124.
18. Norton, P. R.; Griffiths, K.; Bindner, P. E. *Surface Science* **1984,** 138, (1), 125-147.
19. Ronning, M.; Bergene, E.; Borg, A.; Ausen, S.; Holmen, A. *Surface Science* **2001,** 477, (2-3), 191-197.
20. Perdew, J. P.; Burke, K.; Wang, Y. *Physical Review B* **1996,** 54, (23), 16533-16539.
21. Kresse, G.; Hafner, J. *Physical Review B* **1993,** 47, (1), 558-561.
22. Blochl, P. E. *Physical Review B* **1994,** 50, (24), 17953-17979.
23. Monkhorst, H. J.; Pack, J. D. *Physical Review B* **1976,** 13, (12), 5188-5192.
24. Vang, R. T.; Laegsgaard, E.; Besenbacher, F. *Physical Chemistry Chemical Physics* **2007,** 9, (27), 3460-3469.
25. Longwitz, S. R.; Schnadt, J.; Vestergaard, E. K.; Vang, R. T.; Laegsgaard, E.; Stensgaard, I.; Brune, H.; Besenbacher, F. *Journal of Physical Chemistry B* **2004,** 108, (38), 14497-14502.